

Cluster-based Deterioration Prediction of Composite Pavements with Incorporation of Flooding

I. Neema^a, F. Banani Ardecani^a, and O. Shoghli^a

^aDepartment of Engineering Technology and Construction Management,
University of North Carolina at Charlotte, USA

E-mail: ineema1@uncc.edu, fbanania@uncc.edu, oshoghli@uncc.edu

Abstract –

Natural disasters lead to severe deterioration of valuable highway assets, including pavements that should quickly return to service after extreme events such as flooding. Various prediction models were developed to predict pavement performance for several purposes, including maintenance management, budget allocation, and investment strategy. However, limited studies focused on developing a deterioration model for flood-affected composite pavements. This paper proposes a framework for evaluating and predicting the change in composite pavements' roughness due to the flood probability. To this end, a cluster-based pavement deterioration model was developed and applied to a case study of 102 pavement sections from the LTPP database in the United States' eastern region from 2015 to 2019. Then, we used Markov Chain and Monte Carlo simulation on three generated clusters to predict the flood impact on three groups of pavements with different characteristics. The pivotal role of the proposed framework is predicting IRI values due to varying flooding probabilities in different pavement clusters. The results indicate that the pavement tends to deteriorate faster in the initial post-flood years if subjected to heavy or moderate traffic loading and precipitation conditions. This rate will tend to decrease as the age of the pavement increases. For the sections subjected to low traffic loading and low precipitation, the rate of deterioration for the initial post-flood years is less. Still, it will tend to increase as the age of pavement increases.

Keywords –

Pavement deterioration; Markov Chain; Monte Carlo simulation; Composite pavements; LTPP

1 Introduction

Natural disasters and extreme weather events such as flooding, frequent heavy rainfall, and snow contribute to

deterioration in pavement more quickly than normal weather conditions. Some studies have been conducted in the past to understand the impact of flooding on the pavement network [1, 2, 3]. In 2005, two hurricanes, Katrina & Rita, hit New Orleans and the southeastern part of Louisiana in the US, submerging approximately 2,000 miles of road length in flood runoff for five weeks [2]. Highway maintenance management and optimization, especially in the presence of extreme events, are critical [4]. Hence, decision-makers endeavor to develop efficient deterioration models, a key element of maintenance optimization, and establish pre-and-post flood strategies to predict pavement performance under flood conditions to decrease the loss of life and the physical loss of the assets themselves, damage to transport infrastructure, and socio-economic losses. Also, traffic loading, material quality, and surrounding geographical & environmental conditions are among the factors that cause pavement deterioration throughout their lifespan. Due to the fact that these required variables are stochastic, the Markov chain model as a stochastic model can describe the sequence of possible events [5]. Also, various researchers applying the Markov chain theory to construct facilities such as pavements and bridges to predict their deterioration [6, 7, 8, 9] have used the Markov Chain model for predicting pavement deterioration. Although many studies have developed deterioration models, we identified some gaps in the existing frameworks: (1) limited research was conducted on developing probabilistic pavement deterioration models for composite pavement networks. Some of these studies have considered single deterioration models for all the pavement sections; (2) most of the Pavement Management Systems (PMS) used by transportation agencies do not incorporate the effect of flooding in their prediction models.

Considering a single deterioration model for various pavements underestimates or overestimates the pavement condition [10, 11]. Also, when large pavement stretches need to be maintained, prioritizing a particular pavement section's maintenance work becomes complicated. In such a situation, pavement sections' clustering is a

valuable tool for developing a section-wise maintenance strategy [12].

Various clustering algorithms were utilized in the previous studies. Overall, the *K*-means clustering algorithm is easy to apply, accurate, and effective in handling a large amount of data. Also, the *K*-means clustering algorithm was found suitable for unlabeled and non categorized such as LTPP [10, 12, 13].

Furthermore, precipitation and flooding would increase as tropical cyclones' frequency increases [3]. Zhang et al. assessed the effect of the hurricane that occurred in New Orleans. They found a significant difference in the structural strength of pavement between the submerged and non-submerged pavement sections [14]. A recent study was conducted on these flood-affected pavements by Chowdhury et al. to understand pavement's pre-flood and post-flood structural and surface conditions. They developed a deterministic deterioration model and found that pavement tends to lose its strength more rapidly due to flooding [15]. Also, Khan et al. conducted a study on these flood-affected pavements and developed a probabilistic road deterioration model by incorporating flooding effects [6]. To address these challenges, our main research objectives are to create a clustering algorithm to identify pavement sections with similar characteristics and to develop a cluster-based probabilistic deterioration prediction model in composite pavements under different flooding probabilities by leveraging the LTPP data in multiple states.

2 Methodology

We collected the data from the LTPP database, which does not contain the flood-affected pavement sections' information. Then, we grouped pavement sections into three different clusters using the *K*-means clustering algorithm. Then, with the application of Markov chain analysis and Monte Carlo simulation, we developed a pavement deterioration model for each cluster and utilized it to predict the pre-and-post flood IRI (International Roughness Index) values of flood-affected pavement sections. We selected Markov chain, due to the continuous nature of pavement deterioration over time and the fact that the state-space of the deterioration process is finite in number. Furthermore, The Markov chain model focuses on the transition probabilities and the factors responsible for this transition instead of the factors accountable for condition degradation [17]. All these steps are shown in Figure 1. The steps utilized in this research are separately described in the following section.

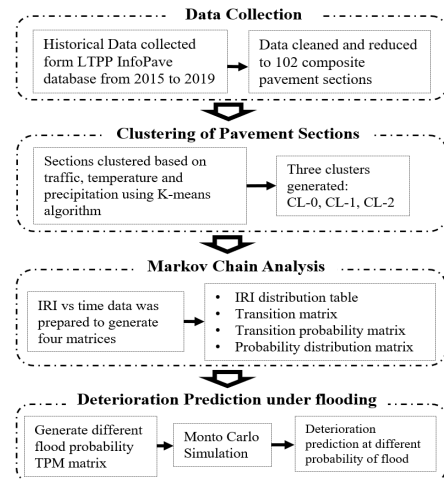


Figure 1. Overall methodology of the analysis

2.1 Data Collection and Clustering

We extracted the IRI, traffic loading (AADTT), temperature, and precipitation data from the LTPP database test sections, belonging to 102 different geographically and spatially composite pavement sections from 2015 to 2019. Figure 2 shows the extent of collected data and their geographical location.

We selected sections data based on three criteria: (1) sections should be composite pavement, (2) sections must be in active monitoring status, and (3) sections should not have maintenance after 2015. The reason behind selecting sections with no maintenance was to remove the improving impact of maintenance (reduction in IRI) in the study. Due to the unavailability of the flood-affected pavement data, we assumed a hypothetical flooding event between 2020 and 2021.



Figure 2. Location of selected pavement sections

It should be noted that all the sections will not follow the same deterioration pattern due to the spatial diversity of collected sections and, in turn, the difference in the contributing factors to their deterioration. To address this issue, we grouped the sections based on the collected historical data (traffic, temperature, and precipitation) using the *K*-means clustering method. The sections within each cluster are homogeneous with each other and heterogeneous between other clusters. Before clustering, we scaled datasets containing traffic, precipitation, temperature, and IRI information between 0 to 1. Then, the *K*-means clustering algorithm was used to cluster the sections. We used the *K*-means method since it is easy to

apply, accurate, and effective in handling a large amount of data [10, 13, 16]. In this study, based on evenly distributing pavement sections, we derived three clusters, CL_0, CL_1 & CL_2, as the optimal number of clusters and as the number of separate deterioration models. Table 1 shows the properties of these clusters.

Table 1. properties of each cluster

Cluster name	Traffic (AADTT)	Temperature (°F)	Precipitation (In)
CL_0	Moderate	Low	High
CL_1	Low	High	Low
CL_2	High	Moderate	Moderate

2.2 Markov Chain Analysis

The Markov chain model is a stochastic model that describes the sequence of possible events. The probability of the next event depends on the current event and not on the event before it [17]. The variables such as traffic loading, environmental aspects, and surface characteristics of the pavements are stochastic. Therefore, we developed the Markov Chain analysis, which comprises four matrices: IRI distribution table, transition matrix, transition probability matrix, and probability distribution matrix. First, we created the IRI distribution table and then developed the other three matrices based on it. The process acquired for developing these matrices is explained below.

2.2.1 IRI Distribution Table

The IRI distribution table was prepared by analysing each section's historical IRI data and then grouping it into each year's respective IRI bucket. A bucket is the IRI range value in m/km. We derived the IRI bucket range based on the following reasons: Pavement sections generally deteriorate with incrementing the IRI value within the range of 0.10 to 0.25 m/km every year [18]. The maximum number of pavement sections in each cluster falls within the IRI range of 0.5 to 1.75 m/km, and due to the low range of the IRI bucket, small changes in the sections were monitored. For uniformly distributing sections into each range bucket, we selected range buckets. The selected IRI bucket range is 0.25 m/km for cluster CL_0 & CL_2, while 0.2 m/km for cluster CL_1; this range is smaller for the cluster CL_1 because more than 90% of the sections have the IRI value less than 1.1 m/km.

2.2.2 Transition Matrix

The transition matrix is an $m \times m$ matrix, where m represents the number of IRI range buckets. This matrix represents the number of sections that will change their IRI value from one range bucket to another in the next year. The IRI data in each cluster were analyzed and

grouped into their respective IRI range bucket for developing the transition matrix. IRI range buckets for cluster CL_0 & CL_2 is 10, while CL_1 is 6. We used the five-year IRI data from 2015 to 2019 of each cluster's sections to develop the transition matrix. We combined the IRI data into four groups, representing the change in IRI between each consecutive year. The pavement sections that show such a decrease in IRI value without any maintenance are not realistic for pavement deterioration, so we did not consider these sections in the analysis.

2.2.3 Transition Probability Matrix

The transition probability is a probability of a pavement section changing its state from the condition i at time t to condition j at time $t + 1$, combined in a matrix called the transition probability matrix (TPM). Several research studies were conducted to derive TPMs using various mathematical methods: the simplest proportion method [19], the expected value method [20], the minimum error method, the percentage transition method, the ordered Probit model, Bayesian technique, and conversion from the deterministic models. In this research, we utilized the percentage transition method. The percentage transition method was feasible for generating the Markov Chain transition probability matrix to derive the change in road condition state with respect to the previous state. This method addresses different explanatory variables used to develop a pavement deterioration model [7]. The transition probability of each pavement section can be calculated using this equation:

$$p_{ij} = \frac{N_{ij}}{N_i} \quad (1)$$

Where p_{ij} is the transition probability from state i to j , N_{ij} is the number of sections transition from state i at time t to state j at time $t + 1$.

For generating the Markov Chain transition probability matrix, we assumed: The condition of the pavement sections cannot be improved without receiving any maintenance treatment, i.e., $p_{ij} = 0$ for $i > j$, the pavement sections which reached their worst condition cannot deteriorate further, i.e., $p_{nn} = 1$, and the pavement section cannot deteriorate by more than one state in a duty cycle.

The TPM is associated with time-independent and time-dependent Markov chain models. This research performed a time-independent Markov chain analysis to develop a pavement deterioration model.

2.2.4 Probability Distribution Matrix

The probability distribution matrix is used to predict the future condition of the pavement at any given year. The pavement network's current condition is termed as

the initial state and described in terms of the initial state vector. The initial state vector of the pavement network is given by [21]:

$$\alpha_0 = [\alpha_1, \alpha_2, \dots, \alpha_n]$$

Initial state vectors assume that all the α_i must be non-negative numbers, and their sum must be equal to one. The TPM is denoted by P and given by [21]:

$$P = \begin{bmatrix} p_{11} & p_{12} & \dots & p_{1n} \\ p_{21} & p_{22} & \dots & p_{2n} \\ \cdot & \cdot & \dots & \cdot \\ \cdot & \cdot & \dots & \cdot \\ p_{n1} & p_{n2} & \dots & p_{nn} \end{bmatrix}$$

Where p_{ij} indicates the probability that a road is currently in state i and will be in state j next year, as the initial state vector, all the TPM numbers must be non-negative, and the sum of each row must be equal to one. The probability distribution of the states at a future time, say $t = 1$ and at time t , may be calculated from the TPM generated and the initial state vector and is shown in equations 1 and 2 [21].

$$\alpha_1 = \alpha_0 P^1 \quad (2)$$

$$\alpha_t = \alpha_0 P^t \quad (3)$$

Where, α_1 is the probability distribution at time $t = 1$, α_t is the probability distribution at time t , α_0 is the initial state vector at time $t = 0$, and P^t is TPM raised to the power of t . In equations (2) and (3), we assumed that the transition probability matrix (P) of the pavement is constant throughout the time; we assumed the deterioration pavement according to this single transition probability matrix P throughout its lifespan. This equation is used for performing time-independent Markov chain analysis. We assumed that the initial condition of the pavement was perfect. $\alpha(0)$ is the initial state vector.

$$\alpha(0) = [1 \ 0 \ 0 \ 0 \ 0 \ 0 \ 0 \ 0 \ 0 \ 0]$$

We generated the probability distribution matrix by substituting the variables $\alpha(0)$ and P^t in equation 3.

2.3 Probabilistic Deterioration Model

The main objective of this research is to generate a probabilistic pavement deterioration model. To this end, we used the Monte Carlo simulation to generate a probabilistic deterioration. In the Monte Carlo simulation, an uncertain variable, roughness (IRI), is assigned multiple values by random variables' intervention to achieve multiple results. The implementation of the Monte Carlo simulation was done by transforming the TPM into a cumulative TPM. In each iteration, we generated 20 uniformly distributed random numbers

between 0 and 1 to have the pavement deterioration model for the next 20 years; we generated 1500 deterioration models. Therefore, we generated 30,000 random numbers in the simulation. These random numbers represent the IRI probability, and we used them to predict future IRI values.

2.4 Modeling Flooding events

We designed a framework (a pavement deterioration model showing a change in the IRI of the pavement surface) for incorporating the effect of different flooding probabilities in the deterioration model. Therefore, we used two types of TPMs: non-flooding TPM and flooding TPM. Both TPMs needed to be developed based on the flood-affected pavement sections' historical IRI data.

For making this framework, we considered these assumptions: (1) the initial pavement condition is excellent, and it was developed based on the year 2020, (2) roughness is majorly affected by the accumulation of flooded water on the pavement surface, (3) the annual flooding probability increases, (4) hypothetical flooding event will occur between the year 2020 and 2021 because the LTPP database does not contain the IRI data of flood-affected pavement sections, (5) for the next 3-4 years rehabilitation work will not be done.

To develop a flood-affected predict model: first, we studied the different flood recurrence intervals: 2-years, 5-years, 10-years, and 20-years. Second, we determined the annual flooding probability for developing a deterioration model. The probability of the above-specified flooding events is 1, 0.5, 0.2, 0.1, and 0.05, respectively. Third, we generated the deterioration model of pavement sections at these specified flooding probabilities. Four, we generated the state vectors representing the transition of the pavement sections into various states. Five, we utilized a set of random numbers, are compared with the flooding probability to determine a non-flooding or flooding TPM; the chance of selecting flooding TPM depends upon the chance of flood occurrence. Six, a second random variable is generated to estimate the pavement's future state. We generated the final pavement state by taking the average of all the simulated states. We repeated this process for 10,000 trials and 20 years to generate the deterioration model for different flooding probabilities.

3 Results

The results derived from the suggested methodology for generating the pavement deterioration model in the previous section are illustrated in this section. We depict sections' IRI value, transition, transition probability, and probability distribution matrix for one of the clusters as an example. Then we compare the results of the deterioration model for the composite pavement with or

without flood affecting all clusters.

3.1 Pavement sections clustering

Figure 3 shows the scatterplot of sections through their cluster identity using their geographical location. Table 2 shows a cluster summary based on each of the cluster's traffic, temperature, and precipitation characteristics. Each cluster comprises sections from various states of the United States.

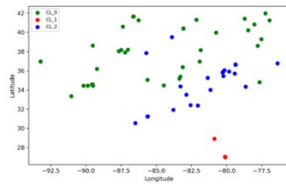


Figure 3. Geographical locations of pavement clusters

Table 2 Section summary of each cluster

cluster name	Number of Sections	Traffic (AADTT)			Temperature (°F)			Precipitation (in)		
		Max	Min	Range	Max	Min	Range	Max	Min	Range
CL_0	44	4748	4	4744	65.8	45.1	20.7	91.3	40.7	50.6
CL_1	14	163	62	101	77.2	71.6	5.6	63.5	31.3	32.2
CL_2	44	5731	17	5714	69.8	52.5	17.3	77.2	34	43.5

3.2 Sections' IRI value

To understand and validate the IRI data quality of each cluster, we prepared the IRI descriptive statistic for each cluster of each year. Table 3 shows The IRI distribution for cluster CL_2. As per the descriptive statistics, sections' IRI value in the specified interquartile range tends to increase every year. It suggests that the pavement sections tend to shift towards the right side of the curve, representing higher IRI values. Higher IRI values represent deterioration in pavement sections. Hence, the IRI data collected showed pavement deterioration and was suitable for developing a deterioration model.

Table 4 shows the IRI distribution table for the CL_0 clusters. This table consists of six columns. The first column represents the IRI bucket range in m/km units. The second column represents the number of sections divided into five sub-sections representing the number of sections in five different years from 2015 to 2019. The third column represents the entire sections, calculated by adding the number of sections each year in a particular range bucket. The fourth column represents the percentage of sections, calculated by taking the summation of total sections in each range bucket and dividing it by the sum of the total sections row. The fifth row represents the cumulative percentage of the sections, calculated by adding the percentage value of the section in each range bucket to the sum of all previous percentage

values. The sixth row represents the lower end range of the bucket. For example, in Table 4, eight sections in the range bucket of 0.5 to 0.75 m/km in 2015, while six sections in 2017 are in the same bucket. The IRI distribution table shows that pavement sections tend to shift in the higher IRI range bucket as time increases. This trend indicates that the IRI of pavement sections is deteriorating with time.

Table 3 IRI descriptive statistics of cluster CL_2

Descriptive statistic	IRI				
	2015	2016	2017	2018	2019
Mean	1.027	1.07	1.141	1.24	1.343
St. Deviation	0.336	0.342	0.344	0.357	0.396
Minimum	0.554	0.55	0.595	0.637	0.665
Maximum	2.126	2.181	2.213	2.561	2.673
25th percentile	0.802	0.837	0.923	1.026	1.085
50th percentile	0.963	1.012	1.063	1.159	1.276
75th percentile	1.206	1.262	1.288	1.438	1.573

Table 4 IRI Distribution table for cluster CL_0

IRI Range (m/km)	Number of Sections					Total Sections	Percent Section	Cumulative Percent	Lower Limit
	2015	2016	2017	2018	2019				
0.500 - 0.750	8	8	6	2	2	26	0.118	0.000	0.500
0.751 - 1.000	15	10	6	2	2	35	0.159	0.118	0.751
1.001 - 1.250	8	11	9	8	7	43	0.195	0.277	1.001
1.251 - 1.500	4	3	9	11	3	30	0.136	0.473	1.251
1.501 - 1.750	3	5	4	8	12	32	0.145	0.609	1.501
1.751 - 2.000	5	4	6	5	7	27	0.123	0.755	1.751
2.001 - 2.250	1	2	3	5	4	15	0.068	0.877	2.001
2.251 - 2.500	0	1	0	1	2	4	0.018	0.945	2.251
2.501 - 2.750	0	0	1	2	3	6	0.027	0.964	2.501
2.751 - 3.000	0	0	0	0	2	2	0.009	0.991	2.751
Total	44	44	44	44	44	220	1.000	1.000	

3.3 Transition Matrix

Table 5 shows the transition matrix for the CL_0 cluster. This table represents the deterioration of pavement sections. Each cell's values represent the number of sections that transitioned its state from one IRI bucket range to another in the next year. This matrix satisfies the requirements of the Markov property, and we further used this matrix in developing the Markov Chain prediction model. In all Transition Matrix tables, the cells showing a zero represent no transition of pavement sections in this IRI bucket range for the next year. For example, in Table 5, 3 pavement sections transitioned from the IRI bucket range of 0.5-0.75 m/km to 0.751-1.0 m/km range, while one sections transitioned from 0.5-0.75 m/km to 1.0-1.250 m/km range.

3.4 Transition Probability Matrix

For developing the transition probability matrix, we used the transition matrix. Table 6 shows the transition probability matrix for the CL_0 cluster. For example, in Table 6, 72.7% of pavement sections remain in the same IRI bucket range of 0.5 – 0.75 m/km for the next year, while 13.6% of pavement sections change their state to

0.751-1.000 m/km IRI range bucket. We used this matrix to develop a probability distribution matrix for a pavement deterioration model in non-flood conditions.

Table 5 Transition Matrix for the Cluster CL_0

IRI Bucket Range (m/km)	Pavement section transition details										
	Number of sections in next year										
Current Year IRI Bucket	0.500-0.750	0.751-1.000	1.001-1.250	1.251-1.500	1.501-1.750	1.751-2.000	2.001-2.250	2.251-2.500	2.501-2.750	2.751-3.000	Total
0.500 - 0.750	16	3	1	0	2	0	0	0	0	0	22
0.751 - 1.000	0	17	9	4	1	2	0	0	0	0	33
1.001 - 1.250	0	0	24	9	2	0	1	0	0	0	36
1.251 - 1.500	0	0	1	12	11	1	2	0	0	0	27
1.501 - 1.750	0	0	0	1	13	6	0	0	0	0	20
1.751 - 2.000	0	0	0	0	0	13	5	1	1	0	20
2.001 - 2.250	0	0	0	0	0	0	6	3	1	1	11
2.251 - 2.500	0	0	0	0	0	0	0	0	3	2	5
2.501 - 2.750	0	0	0	0	0	0	0	0	0	2	3
2.751 - 3.000	0	0	0	0	0	0	0	0	0	2	2

Table 6 Transition Probability Matrix of Cluster CL_0

IRI Bucket Range (m/km)	Transition Probability of Sections										
	Percentage of Sections in Next Year										
Current Year IRI Bucket	0.500-0.750	0.751-1.000	1.001-1.250	1.251-1.500	1.501-1.750	1.751-2.000	2.001-2.250	2.251-2.500	2.501-2.750	2.751-3.000	Total
0.500 - 0.750	0.727	0.136	0.045	0	0.091	0	0	0	0	0	1
0.751 - 1.000	0	0.515	0.273	0.121	0.030	0.061	0	0	0	0	1
1.001 - 1.250	0	0	0.667	0.250	0.056	0	0.028	0	0	0	1
1.251 - 1.500	0	0	0.037	0.444	0.407	0.037	0.074	0	0	0	1
1.501 - 1.750	0	0	0	0.050	0.650	0.300	0	0	0	0	1
1.751 - 2.000	0	0	0	0	0.650	0.250	0.050	0.050	0	0	1
2.001 - 2.250	0	0	0	0	0	0	0.545	0.273	0.091	0.091	1
2.251 - 2.500	0	0	0	0	0	0	0	0	0.600	0.400	1
2.501 - 2.750	0	0	0	0	0	0	0	0	0.667	0.333	1
2.751 - 3.000	0	0	0	0	0	0	0	0	0	1.000	1

3.5 Probability Distribution Matrix

Table 7 shows the probability distribution matrix for the CL_0 cluster and represents the prediction of pavement sections in a particular IRI range bucket. For example, in Table 8, in year 1, 72.7% of sections will remain in the IRI range of 0.5-0.75 m/km, while in year 5, 20.3% of the section will remain this IRI range, and so on forth. After generating these three matrices, the Markovian Chain analysis is completed and used in developing the deterioration model for all the clusters.

3.6 Monte Carlo simulation logic

We compared the random number in each iteration with the cumulative TPM values to find the IRI value of the following year's pavement section. Table 8 shows the cumulative TPM for cluster CL_0.

The IRI range bucket of 0.5 to 0.75 m/km represents the perfectly smooth pavement surface. So, the comparison starts from this IRI range until the cumulative TPM value was greater than the random number; this process continued. The next iteration will start from the same IRI range in which the last iteration

stopped. We continued this procedure for each of the 20 random numbers (number of prediction years) in a trial and repeated for 1500 trials (number of deterioration models). The final deterioration model was generated by taking the average of all the IRI values in their respective year in each iteration.

Table 7 Probability Distribution Matrix of Cluster CL_0

IRI Range (m/km)	Year1	Year2	Year3	Year4	Year5
0.500 - 0.750	0.727	0.529	0.385	0.280	0.203
0.751 - 1.000	0.136	0.169	0.159	0.135	0.107
1.001 - 1.250	0.045	0.101	0.138	0.156	0.157
1.251 - 1.500	0.000	0.032	0.067	0.091	0.105
1.501 - 1.750	0.091	0.132	0.158	0.177	0.191
1.751 - 2.000	0.000	0.036	0.074	0.108	0.135
2.001 - 2.250	0.000	0.001	0.015	0.035	0.057
2.251 - 2.500	0.000	0.000	0.002	0.008	0.015
2.501 - 2.750	0.000	0.000	0.002	0.008	0.018
2.751 - 3.000	0.000	0.000	0.000	0.003	0.012
Total	1.000	1.000	1.000	1.000	1.000

Table 8 Cumulative Transition Probability Matrix for the Cluster CL_0

IRI Bucket Range (m/km)	Cumulative TPM next year									
	0.500-0.750	0.751-1.000	1.001-1.250	1.251-1.500	1.501-1.750	1.751-2.000	2.001-2.250	2.251-2.500	2.501-2.750	2.751-3.000
0.500 - 0.750	0.7273	0.8636	0.9091	0.9091	1	1	1	1	1	1
0.751 - 1.000	0	0.5152	0.7879	0.9091	0.9394	1	1	1	1	1
1.001 - 1.250	0	0	0.6667	0.9167	0.9722	0.9722	1	1	1	1
1.251 - 1.500	0	0	0.037	0.4815	0.8889	0.9259	1	1	1	1
1.501 - 1.750	0	0	0	0.05	0.7	1	1	1	1	1
1.751 - 2.000	0	0	0	0	0	0.65	0.9	0.95	1	1
2.001 - 2.250	0	0	0	0	0	0	0.5455	0.8182	0.9091	1
2.251 - 2.500	0	0	0	0	0	0	0	0	0.6	1
2.501 - 2.750	0	0	0	0	0	0	0	0	0.6667	1
2.751 - 3.000	0	0	0	0	0	0	0	0	0	1

For example, in Table 8, the first random number generated was 0.52. This number was compared with the cumulative TPM value of 0.727, located in the leftmost corner, in the 0.5 to 0.75 m/km IRI range. The random number 0.52 is less than 0.727. Therefore, the IRI transition in the first year did not happen, so we allocated 0.5 to the IRI value in this trial. If the next random number generated was 0.75, it is compared with 0.727, i.e., 0.5 to 0.75 m/km IRI range. The random number 0.75 is greater than 0.727, so the comparison moves to the next IRI range, 0.75 to 1.0 m/km. The cumulative TPM value in this IRI range is 0.864, greater than 0.75; therefore, the comparison stops here, so we allocated 0.751 to the IRI value for the second year. If the third random number again stopped in the same IRI range of 0.75 to 1.0 m/km, the IRI value allocated for the third year would be 0.752. This kind of pattern will continue until a random number stops in a different IRI range.

3.6.1 Results of Deterioration Model with No-flood

Each year's average IRI value is plotted against time

to obtain the deterioration model. Figure 4 shows the deterioration model of each cluster. The trend in Figure 4 for the CL_0 illustrates that the IRI will increase throughout 20 years, representing continuous pavement deterioration. From 2020 to 2025, the IRI of these sections will increase by the average rate of 0.150 m/km each year. After 2026, it will increase by the average rate of 0.135 m/km till 2029; then from 2030, it will increase by the average rate of 0.093 every year till 2034; and then from 2034, it will increase by the average rate of 0.052 m/km every year till 2039. Due to the characteristics of this cluster (heavy precipitation and moderate traffic loading), the increment in the deterioration rate will be highest for this cluster compared to the other two clusters.

The CL_1's roughness value will start at 0.50 m/km in 2020 and reach 1.15 m/km in 2039, representing continuous pavement deterioration over 20 years. From 2020 to 2025, the IRI of these sections will increase by the average rate of 0.02 m/km each year; after 2026, it will increase by the average rate of 0.043 m/km till 2034; and then from 2035, it will increase by 0.030 m/km every year until 2039. Due to the characteristics of this cluster (lower traffic and precipitation), this cluster's deterioration rate is low compared to the other two clusters. However, the deterioration rate will increase as the pavement age increases because of high temperatures.

The CL_2's roughness value will start at 0.585 m/km in 2020 and reach 2.005 m/km in 2039, representing continuous pavement deterioration over 20 years. From 2020 to 2026, the IRI will increase by the average rate of 0.103 m/km each year; after 2026, it will increase by the average rate of 0.067 m/km till 2032; and then from 2033, it will increase by the average rate of 0.057 m/km each year until 2039. Sections in this cluster are subjected to heavy loading conditions; therefore, this trend aligns with expectations. This cluster represents the classic example of a newly constructed pavement. As the age of pavement increases, it tends to deteriorate faster just after its construction, and as the age of pavement increases, the deterioration rate tends to decrease. Hence, this cluster's deterioration rate will be high from 2020 to 2026, and then it will start falling as the year progresses.

3.6.2 Results of Deterioration Model with Flood

Figure 5 shows the predicted roughness by a jump in the IRI value due to hypothetical flooding events of sections in clusters CL_0, CL_1, and CL_2, respectively, at different flooding probabilities between 2020 to 2021. Table 9 shows the hypothetical flooding matrix for the cluster CL_0. For example, in Figure 5, the CL_0 pavement roughness in 2021 will be 1.603 m/km at a 5% probability of flood, while 1.747 m/km at a 50 % probability of flood. The roughness-based deterioration model tends to decrease when post-flood maintenance is applied to the sections; hence, we show roughness

prediction for the first few years at different flooding probabilities. In all clusters of Figure 5, the flood's maximum impact is shown in 2021 because it occurred between 2020 and 2021. This impact tends to reduce as time increases.

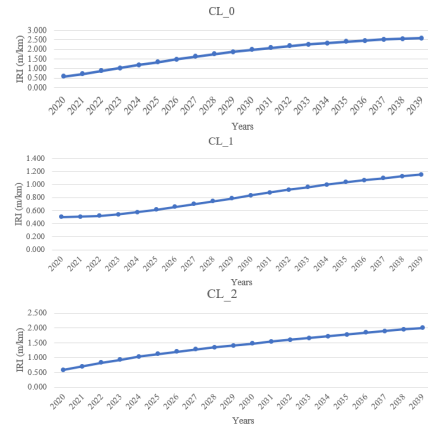


Figure 4. Deterioration Model of the three clusters

Table 9 Hypothetical Flooding TPM for cluster CL_0

Current Year IRI Bucket	Percentage of Sections in Next Year										Total
	0.500 - 0.750	0.751 - 1.000	1.001 - 1.250	1.251 - 1.500	1.501 - 1.750	1.751 - 2.000	2.001 - 2.250	2.251 - 2.500	2.501 - 2.750	2.751 - 3.000	
0.500 - 0.750	0.200	0.8	0	0	0	0	0	0	0	0	1
0.751 - 1.000	0	0.297	0.703	0	0	0	0	0	0	0	1
1.001 - 1.250	0	0	0.48	0.52	0	0	0	0	0	0	1
1.251 - 1.500	0	0	0	0.567	0.433	0	0	0	0	0	1
1.501 - 1.750	0	0	0	0	0.727	0.273	0	0	0	0	1
1.751 - 2.000	0	0	0	0	0	0.611	0.389	0	0	0	1
2.001 - 2.250	0	0	0	0	0	0	0.615	0.385	0	0	1
2.251 - 2.500	0	0	0	0	0	0	0	0.556	0.444	0	1
2.501 - 2.750	0	0	0	0	0	0	0	0	0.444	0.556	1
2.751 - 3.000	0	0	0	0	0	0	0	0	0	1	1

4 Conclusion

The primary objective of this research was to develop a cluster-based probabilistic flood-affected pavement deterioration model for composite pavements. The results indicate that the pavement tends to deteriorate faster in the initial years if subjected to heavy or moderate traffic loading and precipitation condition. This rate will tend to decrease as the age of the pavement increases. Similar trends were shown by the deterioration model of clusters CL_1 and CL_2. Suppose the pavement sections are subjected to low traffic loading and low precipitation. In that case, the rate of deterioration for the initial years is less, but it will tend to increase as the age of pavement increases. Also, the LTPP data illustrate that the impact of flooding on the pavement's roughness is maximum when the probability of flooding is maximum, which confirms the literature.

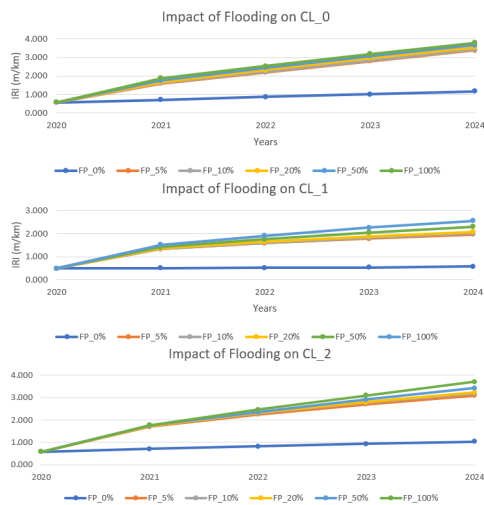


Figure 5. Pavement deterioration model at different probability of flooding for CL_0, CL_1, and CL_2

References

- [1] Lu, D., Tighe, S. L., & Xie, W.-C. International Journal of Pavement Engineering, Impact of flood hazards on pavement performance, 1-7, 2018.
- [2] Sultana, M., Chai, G., Martin, T., & Chowdhury, S. A study on the flood affected flexible pavements in Australia. Paper presented at the 9th international conference on road and airfield pavement technology, 2015.
- [3] Paerl, H. W., Hall, N. S., Hounshell, A. G., Luettich, R. A., Rossignol, K. L., Osburn, C. L., & Bales, J. Recent increase in catastrophic tropical cyclone flooding in coastal North Carolina, USA: Long-term observations suggest a regime shift. Scientific reports, 9(1), 1-9, 2019.
- [4] Shoghli O, De La Garza JM. Multi-Asset Optimization of Roadways Asset Maintenance. In Computing in Civil Engineering (pp. 297-305), 2017.
- [5] Kerali, H., & Snaith, M. NETCOM: the TRL visual condition model for road networks, 1992.
- [6] Khan, M. U., Mesbah, M., Ferreira, L., & Williams, D. J. Developing a new road deterioration model incorporating flooding. Paper presented at the Proceedings of the Institution of Civil Engineers-Transport, 2014a.
- [7] Khan, M. U., Mesbah, M., Ferreira, L., & Williams, D. J. Development of road deterioration models incorporating flooding for optimum maintenance and rehabilitation strategies. Road & Transport Research: A Journal of Australian and New Zealand Research and Practice, 23(1), 3, 2014b.
- [8] Madanat, S., Bulusu, S., & Mahmoud, A. Estimation of infrastructure distress initiation and progression models. Journal of Infrastructure Systems, 1(3), 146-150, 1995.
- [9] Saha, P., Ksaibati, K., & Atadero, R. Developing pavement distress deterioration models for pavement management system using Markovian probabilistic process. *Advances in Civil Engineering*, 2017.
- [10] Sunitha, V., Veeraragavan, A., Srinivasan, K. K., & Mathew, S. Cluster-based pavement deterioration models for low-volume rural roads. International Scholarly Research Notices, 2012.
- [11] Karimzadeh A, Shoghli O, Sabeti S, Tabkhi H. Multi-Asset Defect Hotspot Prediction for Highway Maintenance Management: A Risk-Based Machine Learning Approach. Sustainability. 2022 Apr 21;14(9):4979.
- [12] Sandra, A. K., & Sarkar, A. K. Application of fuzzy logic and clustering techniques for pavement maintenance. Transportation Infrastructure Geotechnology, 2(3), 103-119, 2015.
- [13] Alashwal, H., El Halaby, M., Crouse, J. J., Abdalla, A., & Moustafa, A. A. The application of unsupervised clustering methods to Alzheimer's Disease. Frontiers in computational neuroscience, 13, 31, 2019.
- [14] Zhang, Z., Wu, Z., Martinez, M., & Gaspard, K. Pavement structures damage caused by Hurricane Katrina flooding. Journal of geotechnical and geoenvironmental engineering, 134(5), 633-643, 2008.
- [15] Chowdhury, S., Sultan, M., Chai, G., & Martin, T. A Study on the Flood Affected Flexible Pavements in Australia, 2016.
- [16] Karimzadeh A, Sabeti S, Shoghli O. Optimal clustering of pavement segments using K-prototype algorithm in a high-dimensional mixed feature space. Journal of Management in Engineering. Jul 1;37(4):04021022, 2021.
- [17] Gagniuc, P. A. Markov chains: from theory to implementation and experimentation: John Wiley & Sons, 2017.
- [18] Sayers, M. W. The little book of profiling: basic information about measuring and interpreting road profiles, 1998. Retrieved from
- [19] Wang, K. C., Zaniewski, J., & Way, G. Probabilistic behavior of pavements. Journal of Transportation Engineering, 120(3), 358-375, 1994.
- [20] Jiang, Y., Saito, M., & Sinha, K. C. Bridge performance prediction model using the Markov chain, 1988.
- [21] Ortiz-García, J. J., Costello, S. B., & Snaith, M. S. Derivation of transition probability matrices for pavement deterioration modeling. Journal of Transportation Engineering, 132(2), 141-161, 2006.